

See discussions, stats, and author profiles for this publication at: <https://www.researchgate.net/publication/8673498>

# Shi B, Narayanan TK, Christian BT, Chattopadhyay S, Mukherjee J. Synthesis and biological evaluation of the binding of dopamine D2/D3 receptor agonist, (R,S)-5-hydroxy-2-(N-propyl-...

ARTICLE *in* NUCLEAR MEDICINE AND BIOLOGY · MAY 2004

Impact Factor: 2.41 · DOI: 10.1016/j.nucmedbio.2003.10.004 · Source: PubMed

---

CITATIONS

25

---

READS

6

5 AUTHORS, INCLUDING:



**Bradley T Christian**

University of Wisconsin–Madison

124 PUBLICATIONS 2,079 CITATIONS

SEE PROFILE



**Sankha Chattopadhyay**

Variable Energy Cyclotron Centre

38 PUBLICATIONS 335 CITATIONS

SEE PROFILE



**Jogeshwar Mukherjee**

University of California, Irvine

208 PUBLICATIONS 2,444 CITATIONS

SEE PROFILE

# Synthesis and biological evaluation of the binding of dopamine D2/D3 receptor agonist, (*R,S*)-5-hydroxy-2-(*N*-propyl-*N*-(5'-<sup>18</sup>F-fluoropentyl)aminotetralin (<sup>18</sup>F-5-OH-FPPAT) in rodents and nonhuman primates

Bingzhi Shi<sup>a</sup>, Tanjore K. Narayanan<sup>a</sup>, Bradley T. Christian<sup>a</sup>, Sankha Chattopadhyay<sup>b</sup>,  
Jogeshwar Mukherjee<sup>b,\*</sup>

<sup>a</sup>Department of Internal Medicine/Nuclear Medicine, Kettering Medical Center, Wright State University, Dayton, OH 45429, USA

<sup>b</sup>Brain Imaging Center, Department of Psychiatry and Human Behavior, University of California-Irvine, Irvine, CA 92697, USA

## Abstract

We have synthesized a new fluorinated dopamine D2 receptor agonist, (*R,S*)-2-(*N*-propyl-*N*-(5'-fluoropentyl)amino-5-hydroxytetralin (5-OH-FPPAT). The radiosynthesis of the fluorine-18 analog, <sup>18</sup>F-5-OH-FPPAT was achieved in decay corrected yields of 10 to 15% in specific activities of approx. 1.5 to 2 Ci/μmol. In vitro binding and autoradiographic studies of this new radiotracer have been investigated. Using rat striatal homogenate binding assay, 5-OH-FPPAT exhibited an affinity of IC<sub>50</sub> = 6.95 nM. The octanol-buffer partition coefficient, Log P was found to be 1.60. In vitro autoradiographs in rat brain slices with <sup>18</sup>F-5-OH-FPPAT revealed selective binding to the dopaminergic regions in the striata that was displaceable by sulpiride. This selective binding to the striata was also removed in the presence of the GTP analog, 5'-guanylylimidodiphosphate, indicative of predominant binding of <sup>18</sup>F-5-OH-FPPAT to the high-affinity state of the D2 receptor. In vivo regional distribution of <sup>18</sup>F-5-OH-FPPAT in rat brains revealed selective localization in the striata with striata/cortex ratio of 1.5 and striata/cerebellum ratio of 1.8 to 2.0. The binding of <sup>18</sup>F-5-OH-FPPAT in the striata was reduced upon pretreatment with the antagonist, risperidone and the agonist, PPHT. A PET study in rhesus monkeys showed selective localization of <sup>18</sup>F-5-OH-FPPAT in the striata and the ratio between striata and cerebellum approached approximately 2 at 40 min post-injection. © 2004 Elsevier Inc. All rights reserved.

**Keywords:** <sup>18</sup>F-5-OH-FPPAT; Dopamine D-2 Receptor Agonist; In vitro Autoradiography; PET

## 1. Introduction

There has been a growing interest in the development of positron emitting agonists for imaging dopamine D2 receptors. The agonists are considered to bind preferentially to the high-affinity (HA) state of the receptor that is functionally coupled to G-protein. The HA-state of the receptor is therefore believed to be the functional state since it initiates a cascade of signal transduction pathways and may therefore be an important target in order to image brain activity. Antagonists, such as <sup>11</sup>C-raclopride and <sup>18</sup>F-fallypride are already being studied by PET and allow the measurement of "total receptor concentrations", i.e., HA-state and low-affinity (LA) states of the D2 receptors. A combination of the

antagonist and agonist PET data may allow the evaluation of total receptor concentration and the concentration of the high-affinity receptors. Thus, PET studies may offer new, more comprehensive and more sensitive tools in order to investigate this receptor system.

Efforts to develop a dopamine D2 receptor agonist radiotracer with the potential for non-invasive imaging are being pursued in several laboratories. In recent years, the notion of agonist imaging agents for the dopamine D2 receptor has been realized. We have successfully developed several carbon-11 labeled 5-hydroxy-2-aminotetralins that are D2/D3 receptor agonists and can be used as PET imaging agents [1]. In vivo evaluation of one of these agents, (*R,S*)-2-(*N*-propyl-*N*-(1'-<sup>11</sup>C-propyl)amino-5-hydroxytetralin (<sup>11</sup>C-5-OH-DPAT) in rodents and monkeys has shown the possibility of imaging the HA-states of D2/D3 receptor [2]. Additionally, <sup>11</sup>C-PPHT and <sup>11</sup>C-ZYY339, both of which are higher affinity than <sup>11</sup>C-5-OH-DPAT have also shown

\* Corresponding author. Tel.: +1-949-824-2018; fax: +1-949-824-7873.

E-mail address: mukherjj@uci.edu (J. Mukherjee).

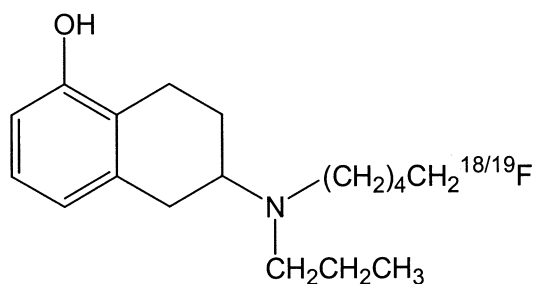


Fig. 1. Chemical structure of (*R, S*)-2-(*N*-propyl-*N*-5'-fluoropentyl)amino-5-hydroxytetralin (5-OH-FPPAT) and (*R, S*)-2-(*N*-propyl-*N*-5'- $^{18}\text{F}$ -fluoropentyl)amino-5-hydroxytetralin ( $^{18}\text{F}$ -5-OH-FPPAT).

the ability to serve as PET imaging agents [3]. Radiolabeling and in vivo distribution studies with apomorphine-based dopaminergic agonists have also been carried out [4–6].

We have now initiated the development of fluorine-18 labeled analogs of 5-OH-DPAT as potential D2/D3 receptor-selective agonists. Previously, efforts have been made towards developing fluorine-18 agents by incorporating a *N*-fluoropropyl group on this molecule that showed poor selectivity in vivo for receptor-rich regions [7]. The electron-withdrawing effects of fluorine on the necessary electronegative nitrogen may have been a potential cause for the poor in vivo properties. This is similar to what has been observed with derivatives of substituted benzamides [8]. Thus, we decided to attenuate the detrimental effects of fluorine by incorporating it at the terminal carbon of a *n*-pentyl group, in order to provide (*R,S*)-2-(*N*-propyl-*N*-5'-fluoropentyl)amino-5-hydroxytetralin (5-OH-FPPAT).

We report here the synthesis and in vitro binding studies of 5-OH-FPPAT. We have also carried out the radiosynthesis of (*R,S*)-2-(*N*-propyl-*N*-5'- $^{18}\text{F}$ -fluoropentyl)amino-5-hydroxytetralin ( $^{18}\text{F}$ -5-OH-FPPAT; Fig. 1) which was then used for in vitro autoradiographic studies in rat brain slices. Additionally, we have evaluated the in vivo binding of  $^{18}\text{F}$ -5-OH-FPPAT to D2/D3 receptors in rodents and the binding of  $^{18}\text{F}$ -5-OH-FPPAT in the monkey brain using PET.

## 2. Materials and methods

All chemicals and solvents were of high grade from Aldrich Chemical Co. Risperidone and PPHT ((*RS*)-2-(*N*-phenethyl-*N*-propyl)amino-5-hydroxytetralin) were purchased from Research Biochemicals Int. Electrospray mass spectra were obtained on a Model 7250 mass spectrometer (Micromass LCT). Proton NMR spectra were acquired on a GE NMR OMEGA 500-MHz or a 500 MHz Bruker-Advance 500 spectrometer to confirm compound structures. Carbon-13 NMR spectra were also obtained on a 90 MHz or 500 MHz Bruker spectrometer (data not shown). High specific activity  $^{18}\text{F}$ -fluoride was produced in the CTI RDS-112 cyclotron using oxygen-18 enriched water target ( $^{18}\text{O}$  to  $^{18}\text{F}$  using p, n reaction). The high specific activity  $^{18}\text{F}$ -fluoride

was used in subsequent reactions. The final reaction mixture was purified by reverse-phase HPLC using a C-18 reverse-phase column eluted with 70% acetonitrile and 0.25% triethylamine in water to provide 5-OH- $^{18}\text{F}$ -FPPAT in specific activities of approximately 2000 Ci/mmol. Fluorine-18 radioactivity was counted in a Capintec dose calibrator while low-level counting was carried out in a well-counter (Auto-Gamma 5000, Packard Instruments Co.). Portions of the radiosynthesis were carried out in the Chemistry Processing Control Unit (CPCU). Radioactive thin layer chromatographs were obtained by scanning in a Bioscan System 200 Imaging scanner (Bioscan, Inc). Autoradiographic studies were carried out by exposing tissue samples on storage phosphor screens. The apposed phosphor screens were read by Cyclone Storage Phosphor System (Packard Instruments Co.). For purposes of comparing the gray and white matter in the brain slices, some of the slides (containing the brain slices) were scanned using a UMAX Mirage II Scanner interfaced to a Silicon Graphics computer (SGI Octane). The slices were scanned at 500 DPI in the gray scale mode and the images were saved as TIF files. All animal studies were approved by the Institutional Animal Care and Use Committee of Wright State University.

### 2.1. Synthesis

#### 2.1.1. (*R,S*)-2-(*N*-propyl-*N*-5'-bromopentanoyl)amino-5-methoxytetralin (2)

(*R,S*)-2-(*N*-propylamino)-5-methoxytetralin (1, 540 mg; 2.46 mmol) was prepared as previously described [1] and acylated using 5-bromovaleryl chloride (560 mg; 2.62 mmol) in 15 mL of methylene chloride in the presence of potassium carbonate (306 mg, 2.2 mmol). The mixture was stirred at ambient temperature for a period of 4 hrs after which the reaction mixture was quenched with saturated sodium bicarbonate solution (20 mL) and extracted with methylene chloride (4 × 20 mL). The organic extract was washed with brine and dried over anhydrous magnesium sulfate. The crude amide was obtained after removal of the methylene chloride under vacuum.

Flash chromatography with 5% ethyl acetate, 50% methylene chloride in hexanes gave a thick oil, 594 mg (60% yield).  $^1\text{H}$  NMR (360 MHz,  $\text{CDCl}_3$ )  $\delta$  0.899 plus 0.933 (2t,  $J = 7.2$  Hz, 3H), 1.56 to 1.72 (m, 3H), 1.78 to 1.99 (m, 5H), 2.32 to 2.44 (m, 2H), 2.55 to 2.86 (m, 2H), 2.90 to 3.20 (m, 5H), 3.418 plus 3.444 (2t,  $J = 6.6$  Hz, 2H), 3.78 (s, 3H,  $\text{OCH}_3$ ), 6.60 to 6.72 (m, 2H, Ar6&8), 7.00 to 7.16 (m, 1H, Ar7). Mass Spectra: 406 (90%), 404 (100%)  $[\text{M}+\text{Na}]^+$ ; 384 (28%), 382 (30%)  $[\text{M}+\text{H}]^+$ .

#### 2.2. (*R,S*)-2-(*N*-propyl-*N*-5'-bromopentanoyl)amino-5-hydroxytetralin (3)

Deprotection of the substituted aminotetralin (2, 530 mg; 1.3 mmol) was carried out using 1.0 M solution of boron tribromide (1.6 mL; 1.6 mmol) similar to previously re-

ported methods [1]. To a chilled solution ( $-30^{\circ}\text{C}$ ) of the methoxytetralin in 5 mL of methylene chloride, boron tri-bromide was added and the mixture was allowed to warm to ambient temperature and stirred for 12 hrs. Subsequently, methanol (2 mL) was added and the mixture was stirred for 2 hrs. The reaction mixture was concentrated under reduced pressure and redissolved in methylene chloride (60 mL), washed with saturated sodium bicarbonate solution, water, brine, dried over anhydrous magnesium sulfate, concentrated to yield a crude product mixture.

Flash chromatography with 1.2% methanol, 0.01% triethylamine, 2% ethyl acetate, 40% hexanes in methylene chloride gave a thick oil 325 mg (64% yield).  $^1\text{H}$  NMR (360 MHz,  $\text{CDCl}_3$ )  $\delta$  0.896 plus 0.938 (2t,  $J = 7.2$  Hz, 3H), 1.42 to 1.77 (m, 4H), 1.80 to 1.93 (m, 4H), 2.35 to 2.45 (m, 2H), 2.55 to 2.99 (m, 2H), 3.00 to 3.20 (m, 5H), 3.359 plus 3.397 (2t,  $J = 6.8$  Hz, 2H), 6.54 to 6.75 (m, 2H, Ar6&8), 6.89 to 7.01 (m, 1H, Ar7). Mass Spectra: 390, 392 (3%)  $[\text{M}+\text{Na}]^+$ , 368, 370 (5%)  $[\text{M}+\text{H}]^+$ .

### 2.3. (*R,S*)-2-(*N*-propyl-*N*-5'-bromovaleryl)amino-5-tetrahydropyranyltetralin (4)

To a stirred solution of the hydroxytetralin (3, 104 mg; 0.28 mmol) in 15 mL of methylene chloride was added a catalytic amount of toluenesulfonic acid (12 mg, 0.056 mmol) followed by addition of dihydropyran (40  $\mu\text{L}$ ; 0.44 mmol) at ambient temperature. The reaction mixture was stirred for 24 h, quenched with a saturated sodium bicarbonate solution (20 mL), extracted with methylene chloride ( $3 \times 20$  mL), dried over anhydrous magnesium sulfate, concentrated to yield a crude product.

Flash chromatography with 1% methanol, 0.01% triethylamine, 2% ethyl acetate, 25% methylene chloride in hexanes gave a thick oil 58 mg (46% yield).  $^1\text{H}$  NMR (500 MHz,  $\text{CDCl}_3$ )  $\delta$  0.89 to 0.95 (m, 3H), 1.55 to 1.98 (m, 14H), 2.35 to 2.45 (m, 2H), 3.40 to 3.60 (m, 5H), 4.60 to 4.68 (br, 1H), 4.90 to 4.96 (m, 1H), 6.57 to 6.67 (m, 2H, Ar6&8), 6.92 to 7.05 (m, 1H, Ar7). Mass Spectra: 390, 392 (3%)  $[\text{M}+\text{Na}-\text{C}_5\text{H}_9\text{O}]^+$ , 372 (68%)  $[\text{M}-\text{HBr}]^+$ , 289 (75%)  $[\text{M}-\text{C}_5\text{H}_9\text{O}-\text{Br}]^+$ , 288 (86%)  $[\text{M}-\text{C}_5\text{H}_9\text{O}-\text{HBr}]^+$ .

### 2.4. (*R,S*)-2-(*N*-propyl-*N*-5'-fluoropentyl)amino-5-hydroxytetralin (5a)

(*R,S*)-2-(*N*-propyl-*N*-5'-bromopentanoyl)amino-5-hydroxytetralin (3, 30 mg, 0.08 mmol) was reacted with tetrabutylammonium fluoride (2 mL, 1.0 M in THF) and 20 equivalents of potassium fluoride for 24 hrs. The reaction mixture was quenched with water (20 mL), extracted with methylene chloride ( $4 \times 15$  mL), dried over anhydrous magnesium sulfate, concentrated to yield a crude product. This crude product was then taken up in anhydrous THF and to this solution at ambient temperature, lithium aluminum hydride (0.1 mL, 1.0 M in THF) was added. The reaction was stirred for 2 hrs. Following the reaction, the reaction mixture was quenched with brine (15 mL), extracted with

methylene chloride ( $3 \times 15$  mL), dried over anhydrous magnesium sulfate and concentrated to yield a crude product.

The crude product was then purified using preparative TLC to provide 7 mg of the pure product (29% yield).  $^1\text{H}$  NMR (500 MHz,  $\text{CDCl}_3$ )  $\delta$  1.02 (t, 3H), 1.40 to 1.80 (m, 10H), 2.40 to 2.55 (m, 4H), 2.90 to 3.15 (m, 5H), 4.53 to 4.41 (dt, 2H,  $\text{CH}_2\text{F}$ ), 6.58 (d, 1H, Ar6), 6.84 (d, Ar8), 6.96 (t, 1H, Ar7). Mass Spectra: 294 (100%)  $[\text{M}+\text{H}]^+$ , 274 (14%)  $[\text{M}-\text{F}]^+$ , 256 (8%)  $[\text{M}-\text{C}_3\text{H}_7]^+$ .

## 2.5. Radiosynthesis

### 2.5.1. (*R,S*)-2-(*N*-propyl-*N*-5'- $^{18}\text{F}$ -fluoropentyl)amino-5-hydroxytetralin (5b)

High specific activity fluorine-18 from the RDS cyclotron was delivered to the CPCU. Using modifications of the FDG synthesis program, the precursor, (*R,S*)-2-(*N*-propyl-*N*-5'-bromopentanoyl)amino-5-tetrahydropyranyltetralin 3, was used. Fluorine-18 was solubilized using Kryptofix and potassium carbonate and evaporated to dryness using anhydrous acetonitrile. Subsequently, the bromo precursor 3 (2 mg in 1 mL of anhydrous acetonitrile) was added and the reaction went for 20 min at  $96^{\circ}\text{C}$ . Following the reaction, methanol was added to the mixture and the methanolic contents were passed through a neutral alumina seppak (prewashed with methanol) out of the CPCU. This removed any unreacted  $^{18}\text{F}$ -fluoride and the methanolic solution now contained (*R,S*)-2-(*N*-propyl-*N*-5'- $^{18}\text{F}$ -fluoropentanoyl)amino-5-tetrahydropyranyltetralin. The methanol was removed *in vacuo*, and to the residue was added lithium aluminum hydride (0.2 mL of 1.0 M LAH in THF) in order to reduce the amide. The reaction was allowed to go for 2 mins at room temperature. Subsequently, hydrochloric acid (0.6 mL of 0.7 N HCl) was added to quench the unreacted LAH and to deprotect the tetrahydropyran. The reaction proceeded at  $80^{\circ}\text{C}$  for 15 mins. The contents were then cooled to ambient temperature, quenched with 0.8 mL of 1.0 M sodium bicarbonate solution, extracted with methylene chloride. The organic extract was evaporated and the residue was taken up for HPLC purification. The retention time of  $^{18}\text{F}$ -5-OH-FPPAT was found to be 13.5 mins using the solvent of 68% acetonitrile, 0.25% triethylamine in water at a flow rate of 3.0 mL/min. The radiosynthesis was accomplished in 2 hrs from end of bombardment with a decay corrected overall radiochemical yield of 10 to 15%. The specific activity of the radiotracer was estimated to be 1500 to 2000 Ci/mmol.

Partition of  $^{18}\text{F}$ -5-OH-FPPAT between octanol and 0.066 M phosphate buffered saline, pH 7.4 was carried out in order to estimate lipophilicity of  $^{18}\text{F}$ -5-OH-FPPAT similar to procedures described previously [1]. The log P of  $^{18}\text{F}$ -5-OH-FPPAT was found to be  $1.60 \pm 0.02$ .

## 2.6. In vitro binding assays

Male Sprague-Dawley rats (200 to 250 g) were sacrificed and the brain homogenate prepared as previously described

[1]. The  $IC_{50}$  for inhibition of  $^{18}F$ -fallypride binding to striatal homogenate was determined as follows: To start the incubation, 0.5 mL of the tissue homogenate was added to each ice-cold assay tube containing  $^{18}F$ -fallypride and the displacing ligand at a final concentration ranging from 0.1 pM to 100  $\mu$ M with a final volume of 1 mL. Nonspecific binding was determined at a concentration of 10  $\mu$ M sulpiride. After addition of tissue, the tubes were removed from the ice, vortexed for 3 s and incubated at 37°C for 60 min. The incubation was terminated by filtration through Whatman GF/B filters presoaked in 0.3% polyethylenimine, with a Brandel model M-24R cell harvester. The filters were rinsed for 10 s with ice-cold Tris-HCl buffer, and the filters were counted using for 511 Kev decay of fluorine-18 using a Auto-Gamma 5000 (Packard Instruments Co.). This fluorine-18 data was decay corrected and subsequently analyzed using Ligand (Biosoft Inc.) and  $IC_{50}$  values for the various drugs were obtained.

### 2.7. *In vitro* autoradiographic studies

Rat brain tissue sections (obtained as previously described in [2] were removed from storage and were allowed to come to room temperature (22 to 25 °C) over a period of 15 to 30 min. The tissue sections were placed in 50 mM Tris HCl buffer (pH 7.4, 25 °C) containing 120 mM NaCl and 5 mM KCl and were preincubated for 15 min. The slices were then incubated in fresh buffer with  $^{18}F$ -5-OH-FPPAT at concentrations of approximately 1 nM for 60 min at 25°C for total binding. In the case of experiments with 5'-guanylylimidophosphate (Gpp(NH)p), which is known to convert the HA-sites to LA-sites [9], brain slices were preincubated for 15 mins at 25°C with the above mentioned buffer containing 33  $\mu$ M of Gpp(NH)p and subsequently  $^{18}F$ -5-OH-FPPAT was added. Non-specific binding was defined as the binding remaining in the presence of 10  $\mu$ M (*S*)-sulpiride. Following incubation, tissue sections were briefly washed twice for 1 min period each with cold 50 mM Tris HCl buffer, pH 7.4, followed by a quick rinse in cold deionized water. After washing, tissue sections were dried under a cool stream of air. Tissue sections were then apposed to storage phosphor screens (Packard Instruments Co.) and left for overnight exposure. Autoradiograms were read and analyzed using the Cyclone Storage Phosphor System (Packard Instruments Co.).

### 2.8. *In vivo* distribution studies in rats

A group of male Sprague-Dawley rats (200 to 250 g; anesthetized with diethyl ether) were administered with  $^{18}F$ -5-OH-FPPAT (100  $\mu$ Ci in 0.15 mL) via an intracardiac injection. The groups of rats were sacrificed at 15, 30 and 60 mins post-injection of  $^{18}F$ -5-OH-FPPAT and the brain was rapidly isolated and the various regions such as striata, cortex and cerebellum were dissected. These regions were counted for fluorine-18 radioactivity and weighed in order to compute % injected dose/g of  $^{18}F$ -5-OH-FPPAT.

Drug challenge studies were carried out with the D-2 receptor agonist, PPHT (0.5 mg/kg) and antagonist, risperidone (0.5 mg/kg). The drugs were administered intraperitoneally, 15 mins prior to the administration of the radiopharmaceutical. The rats were then administered with the radiopharmaceutical,  $^{18}F$ -5-OH-FPPAT (100  $\mu$ Ci in 0.10 mL injected intracardially) under anesthesia (exposure to ether vapors) and subsequently allowed free access to food and water. All rats were killed 30 mins after the administration of the radiopharmaceutical and the brain was rapidly isolated and the various regions such as striata, cortex and cerebellum were dissected, counted for fluorine-18 radioactivity and weighed to compute % injected dose/g of  $^{18}F$ -5-OH-FPPAT.

### 2.9. PET scans of monkeys

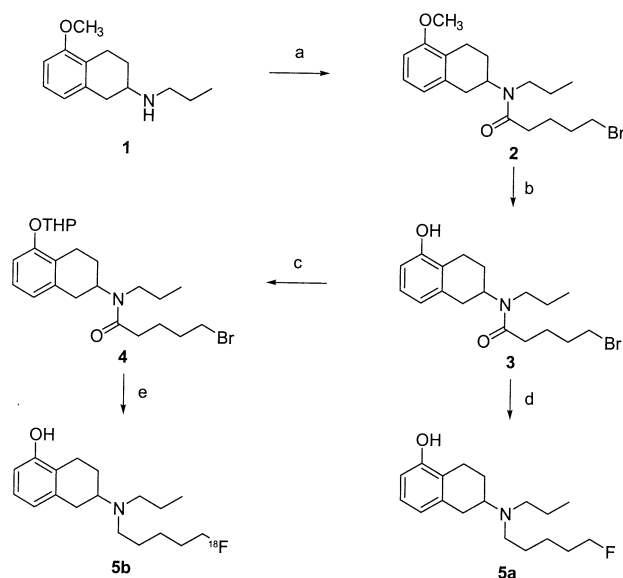
The rhesus monkeys were anesthetized using ketamine (10 mg/kg), xylazine (0.5 mg/kg) and subsequently maintained on 0.5 to 1.5% isoflurane. Two intravenous catheters were placed, one on each arm, for purposes of administration of the radiopharmaceutical and for obtaining blood samples during the study. The head of the animal was placed in the gantry of a Siemen's ECAT CTI HR+ scanner and positioned in place with the use of adhesive tape. After initial positioning the animal was immobilized for the duration of the scan. Image slices of the whole brain were acquired parallel to the canthomeatal plane in 3-D mode. A transmission scan using a Ge-68/Ga-68 rod source was acquired prior to administration of the radiopharmaceutical to correct for tissue attenuation of the coincident radiation. Typically, a dynamic scan of approximately 120 min duration was acquired immediately after administering  $^{18}F$ -5-OH-FPPAT (approximately 3 mCi, iv).

The raw data was reconstructed into a 128 × 128 image matrix (1.7×1.7×2.4 mm pixel size) via an iterative ordered subsets expectation maximization (OSEM) algorithm. The counts in each pixel in the image were then converted to units of percent-injected-dose-per-unit-volume as previously described (Mukherjee et al., 2000). An area showing maximal radioligand binding within the striata, thalamus and cortex was delineated in the images. An area in the cerebellum was chosen for measurement of non-specifically bound radioligand. Specific binding was obtained by subtracting the measured  $^{18}F$ -5-OH-FPPAT binding in the cerebellum from the total measured binding in the striata.

## 3. Results

### 3.1. Synthesis

Synthesis of 5-OH-FPPAT was achieved by following the general pathway for producing aminotetralin derivatives as reported previously [1] and is shown in Fig. 2. The intermediate, 5-methoxy-2-(*N*-propylamino)tetralin 1 was



a. 5-bromovaleryl chloride; b.  $\text{BBr}_3$ ; c. DHP; d.  $\text{Bu}_4\text{NF}$ ,  $\text{KF}$ ; e. 1.  $\text{K}_2^{222}\text{F}^{18}\text{F}$ , 2.  $\text{LiAlH}_4$ , 3.  $\text{HCl}$

Fig. 2. Synthesis scheme of 5-OH-FPPAT and  $^{18}\text{F}$ -5-OH-FPPAT.

prepared as reported (Shi et al., 1999). The inclusion of the 5'-fluoropentyl group was accomplished by first making a 5'-bromopentanoyl derivative 2 of the methoxytetralin 1 in modest yields (60%). Demethylation using boron tribromide of this derivative provided an intermediate 2-(*N*-propyl-*N*-5'-bromovaleryl)amino-5-hydroxytetralin 3 in 64% yield that was used for the production of unlabeled fluorinated derivative. The unlabeled fluorinated derivative 5a was produced in low yields (29%) by treating the bromo-compound 3 with tetrabutylammonium fluoride followed by reduction of the amide with LAH to provide 5-OH-FPPAT,

5a. For purposes of radiolabeling with fluorine-18, the precursor 2-(*N*-propyl-*N*-5'-bromovaleryl)amino-5-tetrahydropyranyltetralin 4 was prepared in which the phenolic group was protected as the tetrahydropyranyl ether.

### 3.2. Radiosynthesis

Radiolabeling with fluorine-18 was accomplished using a fluorine-18 for bromine exchange on the precursor 2-(*N*-propyl-*N*-5'-bromovaleryl)amino-5-tetrahydropyranyltetralin 4. The intermediate 4 was reacted with  $^{18}\text{F}$ -fluoride to provide the radiolabeled amide in the automated CPCU. Subsequent steps of reduction of the amide with LAH followed by deprotection with mild acid were carried out manually outside the CPCU. The reduction and deprotection are rapid and do not add excessive time to the radiolabeling process. However, due to a significant amount of solids and emulsification in the last step, it was necessary to extract the product from the reaction mixture into dichloromethane prior to HPLC purification. The reaction mixture extract was then purified on reverse phase HPLC to obtain the final product appearing at approximately 14 mins, as shown in Fig. 3. No other major radioactive peak was observed in the HPLC. Radiochemical yields of  $^{18}\text{F}$ -5-OH-FPPAT were in the 10 to 15% range decay corrected, and specific activities ranged from 1500 to 2000 Ci/mmol.

### 3.3. In vitro binding studies

Affinity of 5-OH-FPPAT was measured using competition with  $^{18}\text{F}$ -fallypride and compared with that of 5-OH-DPAT and PPHT. Table 1 lists the binding affinity and lipophilicity of 5-OH-DPAT, 5-OH-FPPAT and PPHT. A two-site fit of the binding data resulted in a  $\text{IC}_{50}$  of 6.95 nM for site 1 for 5-OH-FPPAT. This affinity was very similar to the affinity of 5-OH-DPAT ( $\text{IC}_{50}$  of 6.53 nM for site 1). The

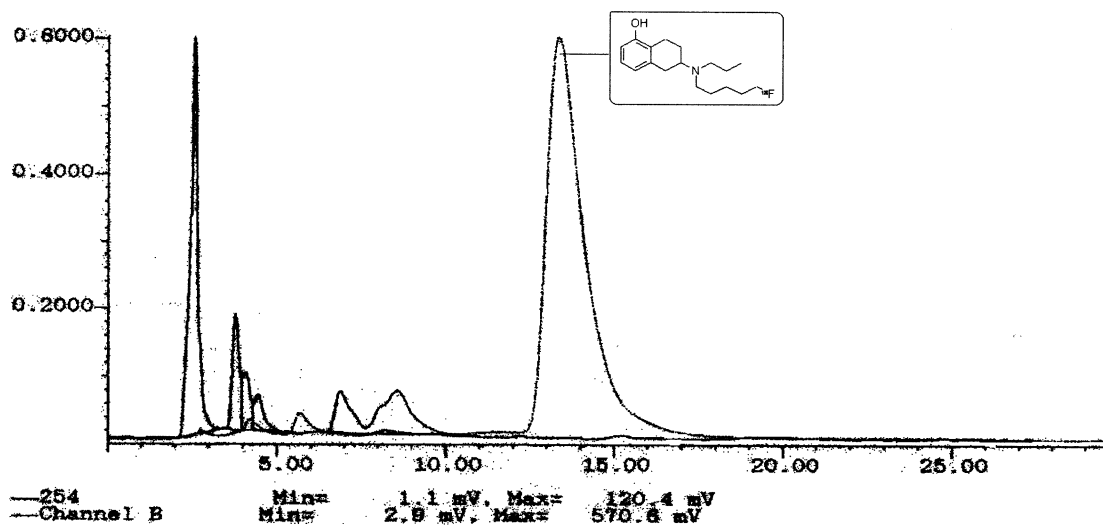


Fig. 3. Reverse phase HPLC chromatogram showing separation profile of  $^{18}\text{F}$ -5-OH-FPPAT on a  $\text{C}_{18}$  reverse phase HPLC column. The predominant radioactive peak at 13.5 min is  $^{18}\text{F}$ -5-OH-FPPAT.

Table 1

*In vitro* affinity and lipophilicity of 5-OH-DPAT, 5-OH-FPPAT and PPHT

Compound	Binding Affinity <sup>a</sup> IC <sub>50</sub> , nM	Lipophilicity <sup>b</sup> Log P
5-OH-DPAT	6.53	1.37
5-OH-FPPAT	6.95	1.60
PPHT	1.74	3.03

<sup>a</sup> Binding affinity measured by using <sup>18</sup>F-fallypride in rat striatal homogenates,

<sup>b</sup> Lipophilicity measured by partitioning the compounds between *n*-octanol and phosphate buffer at pH 7.4.

affinity of PPHT was found to be higher (IC<sub>50</sub> of 1.74 nM for site 1) as expected [1]. Also as expected, 5-OH-FPPAT was found to be more lipophilic (log *P* = 1.60) compared to 5-OH-DPAT (log *P* = 1.37).

### 3.4. *In vitro* autoradiography

Selective binding of <sup>18</sup>F-5-OH-FPPAT was observed in the striata *in vitro* in rat brain slices (Fig. 4). The binding observed in the striata in Fig. 4b was clearly evident and corresponded to the histology of the same slice seen in Fig. 4a. Little specific binding was observed in the cortical areas (Fig. 4b). Cerebellum showed little binding and served as a nonspecific binding region. Specific to nonspecific binding ratios computed for brain slice shown in Fig. 4b were as follows: striata/cerebellum = 17.4; cortex/cerebellum = 1.35 and striata/cortex = 12.8. Sulpiride (10 μM) was able to block in excess of 90% of the selective binding of <sup>18</sup>F-5-OH-FPPAT in the striata (observed in Fig. 4c). In order to evaluate binding of <sup>18</sup>F-5-OH-FPPAT to the high-affinity states, effect of 5'-guanylyl-imidophosphate (Gpp(NH)p) was evaluated. Brain slices that were incubated with 33 μM of Gpp(NH)p had significantly decreased (~70 to ~80%) binding of <sup>18</sup>F-5-OH-FPPAT to the D2 receptors (Fig. 4d). Some residual selective binding remained after

Gpp(NH)p pretreatment consistent with previous observations with agonists (such as [<sup>123</sup>I]S(-)-5-OH-PIPAT, [10].

### 3.5. *In vivo* rodent studies

Binding of <sup>18</sup>F-5-OH-FPPAT was evaluated in Sprague-Dawley rats at different time intervals after the administration of the radiopharmaceutical (Fig. 5a). Binding of <sup>18</sup>F-5-OH-FPPAT was found preferentially in the striata (approximately 1.65% injected dose/g at 15 min postinjection). Cortical regions showed significant amounts of non-specific binding (approximately 80% of that found in the striata at 15 min) as can be seen in Fig. 5a. Significant levels of activity were also found in the cerebellum. Rapid clearance of <sup>18</sup>F-5-OH-FPPAT was observed from all brain regions including the striata. At 30 mins, the ratio of striata to cerebellum = 1.86 which increased to 2 at 60 min postinjection. Cortex to cerebellum ratio was found to be approx. 1.28 and 1.35 at 30 and 60 min postinjection, respectively.

In a separate study, groups of rats were administered <sup>18</sup>F-5-OH-FPPAT, post administration of risperidone (0.05 mg/kg) or PPHT (0.1 mg/kg) and results are shown in (Fig. 5b). Both risperidone and PPHT reduced the binding of <sup>18</sup>F-5-OH-FPPAT, with specific binding reduced to 40% compared to controls, for both risperidone and PPHT.

### 3.6. PET studies with <sup>18</sup>F-5-OH-FPPAT

Binding studies of <sup>18</sup>F-5-OH-FPPAT were carried out in rhesus monkeys (8 to 10 kg). A set of transaxial brain slices of a rhesus monkey injected with <sup>18</sup>F-5-OH-FPPAT are shown in Fig. 6. Images were summed between 8.5 to 30 min postinjection of <sup>18</sup>F-5-OH-FPPAT. Selective binding of <sup>18</sup>F-5-OH-FPPAT was clearly evident in dopaminergic regions such as the caudate and putamen. Additionally, thalamus also indicated a significant amount of binding.

Brain uptake reached levels of approximately 0.05% injected dose per cc in the rhesus monkeys, and the tracer initially accumulated in the striata and cleared from non-

A. Brain slice; 0.01 mm    B. Control    C. 10 μM Sulpiride    D. 33 μM Gpp(NH)p



Fig. 4. *In vitro* autoradiographs of rat brain slices showing the binding of <sup>18</sup>F-5-OH-FPPAT (a). A 10 micron thick rat brain transaxial slice (b). *In vitro* total binding of <sup>18</sup>F-5-OH-FPPAT to this brain slice, (c). Nonspecific binding was measured in the presence of 10 μM sulpiride, and (d). *In vitro* binding in the presence of 33 μM Gpp(NH)p.



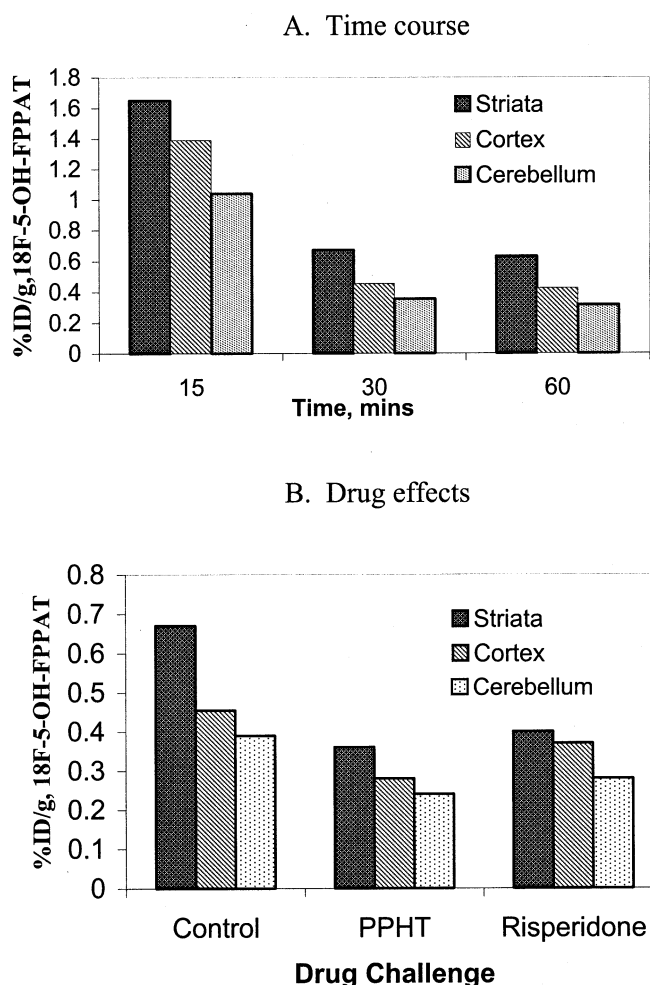


Fig. 5. a. Distribution of  $^{18}\text{F}$ -5-OH-FPPAT in the rat brain regions (striata, cortex and cerebellum) at different time points following administration of the radioligand (data is average of 3 rats for each time-point). b. *In vivo* distribution of  $^{18}\text{F}$ -5-OH-FPPAT in control rats and pretreated rats (3 rats per group) with PPHT (D2-agonist) and risperidone (D2-antagonist).

specifically bound cortical and cerebellar regions. Fig. 7 shows the time-activity curves of  $^{18}\text{F}$ -5-OH-FPPAT binding in the putamen, caudate, thalamus, cortex and cerebellum. Cortical levels of  $^{18}\text{F}$ -5-OH-FPPAT were somewhat similar to that observed in the cerebellum. The binding of  $^{18}\text{F}$ -5-OH-FPPAT peaked at approximately 10 to 15 mins after injection and began to clear rapidly from all brain regions. Dopaminergic regions, such as caudate and putamen showed a slower clearance than cortex and cerebellum. Ratio  $^{18}\text{F}$ -5-OH-FPPAT binding in striata compared to cerebellum exceeded 1.5 after approximately 10 mins and reached a maximum of approximately 2 around 40 mins postinjection. Thalamus to cerebellum ratios were lower (approx. 1.4 at 40 mins).

#### 4. Discussion

The 5-hydroxy aminotetralins are known D2-like receptor agonists. We have previously radiolabeled several de-

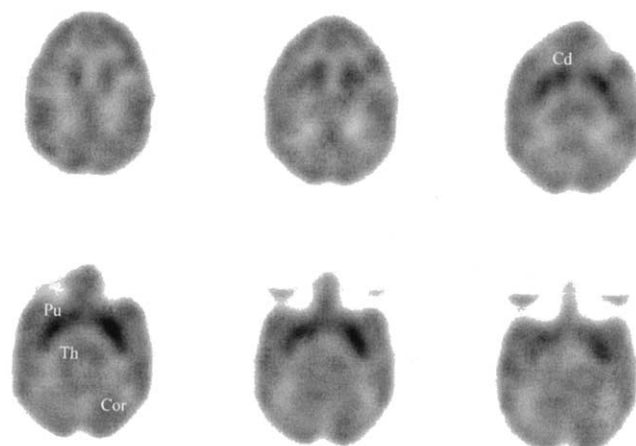


Fig. 6. 2.4 mm thick brain slices from a PET study of a rhesus monkey post-injection of  $^{18}\text{F}$ -5-OH-FPPAT (approx. 2 mCi). Localization of  $^{18}\text{F}$ -5-OH-FPPAT in the caudate (Cd) and putamen (Pu) is seen clearly in most of the slices, while some binding in the thalamus (Th) and cortical regions (Cor) is also seen.

rivatives with carbon-11 [1]. Our preliminary results on these derivatives indicates the ability of *in vivo* imaging of these agonists [2, 3]. Our *in vitro* results with these agents suggest binding to the HA-state of the receptors. In order to take advantage of the longer half-life of fluorine-18 (110 min) over that of carbon-11 (20 min), we have now successfully developed  $^{18}\text{F}$ -5-OH-FPPAT as a potential imaging agent for HA-state D2/D3 receptors.

Since the nitrogen of the aminotetralins is essential for interaction with the aspartate residue in the D2-receptors, we intended to retain its basicity by attenuating the effects of fluorine. Towards this goal we included a *N*-fluoropentyl group while conserving one essential *N*-propyl group. Synthesis of 5-OH-FPPAT was accomplished using some of our previously described procedures [1]. In order to include a fluoropentyl group on the nitrogen, we used the reactive 5-bromovaleryl chloride. This provided the corresponding amide which now contained a bromine atom for inclusion of

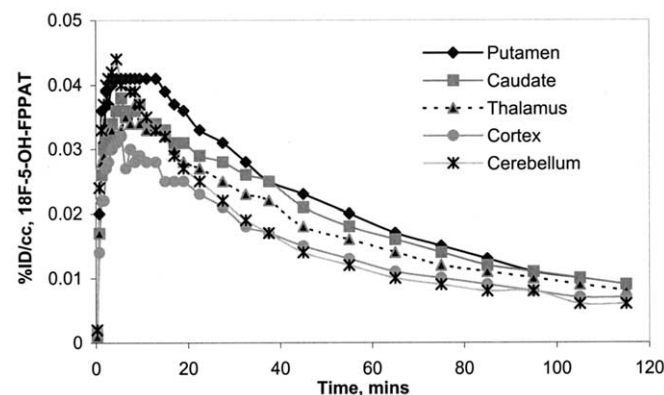


Fig. 7. Time-activity curve of the binding of  $^{18}\text{F}$ -5-OH-FPPAT in the various brain regions (caudate, putamen, thalamus, cortex and cerebellum) of the rhesus monkey after iv administration.



the fluorine. The synthesis of 5-OH-FPPAT was achieved in modest yields by fluorination (fluoride for bromide exchange) followed by reduction of the amide group. Improvements in the yields of 5-OH-FPPAT will be explored by carrying out the fluorination/reduction more efficiently.

For radiolabeling purposes, the phenolic group in the precursor was protected as a tetrahydropyranyl (THP) ether since a free phenolic group interfered in the radiolabeling process. The methoxy group was not a suitable protecting group for the phenol because of inefficient deprotection and loss of the fluorine-18 radiolabel caused by boron tribromide. The  $^{18}\text{F}$ -fluoride for bromide exchange proceeded efficiently on the THP ether. After the reduction and deprotection steps, modest yields of  $^{18}\text{F}$ -5-OH-FPPAT were obtained. Further improvements in the radiosynthesis may involve using a precursor that avoids the reduction step. High specific activity (approx. 1500 to 2000 Ci/mmol) of  $^{18}\text{F}$ -5-OH-FPPAT was obtained after HPLC purification for in vitro studies.

The binding affinity of 5-OH-FPPAT was measured using  $^{18}\text{F}$ -fallypride. The affinity of 5-OH-FPPAT was found to be comparable to that of 5-OH-DPAT and weaker than PPHT. The ability of the D2 receptor to tolerate longer alkyl groups at the receptor site is known [8]. The maximum tolerated length of the carbon chain is about 6 before the affinity decreases significantly. Our goal was to increase the chain length in order to minimize the detrimental effects of fluorine as much as possible. Since fluorine can have some influence up to four carbons away, the five-carbon chain was selected. Our results suggest that inclusion of the longer fluoroalkyl groups has only a small detrimental effect on the binding affinity. It may be worthwhile to study the six-carbon fluoroalkyl chain to see if the binding affinity is improved. The improved lipophilicity of 5-OH-FPPAT over that of 5-OH-DPAT (log *P* 1.60 vs. 1.37) suggests a greater uptake in the brain with  $^{18}\text{F}$ -5-OH-FPPAT compared to  $^{11}\text{C}$ -5-OH-DPAT.

In vitro autoradiographic studies showed selective binding of  $^{18}\text{F}$ -5-OH-FPPAT to the striata (Fig. 4b), which was displaced both by sulpiride, a D2 receptor antagonist (Fig. 4c, showing approx. 90% displacement of bound  $^{18}\text{F}$ -5-OH-FPPAT). Binding to the HA-state of the D2 receptor was confirmed by preincubating the rat brain slices with Gpp(NH)p (Fig. 4d). This guanine nucleotide analog has been previously shown to convert HA-states of the D2 receptor to LA-states [11]. Brain slices that were preincubated with Gpp(NH)p exhibited significantly lower (Fig. 4d, showing approx. 74% reduction of  $^{18}\text{F}$ -5-OH-FPPAT binding). This is indicative of little or no binding to the LA-state of the D2 receptor. Thus, these experiments confirmed the binding of  $^{18}\text{F}$ -5-OH-FPPAT to the HA-state of the D2 receptor in vitro. These findings are similar to those obtained with  $^3\text{H}$ -PHNO, where it was shown that Gpp(NH)p decreased or abolished the binding of  $^3\text{H}$ -PHNO to the D2 receptors in rat brain slices in vitro [11]. The residual binding may be due to incomplete conversion of the affinity states, some

binding to the low affinity states or possible internalization of the receptor-ligand complex.

In order to show selectivity and the ability of  $^{18}\text{F}$ -5-OH-FPPAT to bind to the D2 receptors in vivo, rat in vivo experiments were carried out. Fig. 5a shows the distribution of  $^{18}\text{F}$ -5-OH-FPPAT in the various rat brain regions to be fairly high at 15 mins post-injection. The striata exhibited about 1.65% injected dose/g which was more than cortex and cerebellum. The kinetics in all the brain regions are relatively fast, which is consistent with our previous observations with  $^{11}\text{C}$ -5-OH-DPAT. Selectivity in the binding to the striata was evident with striata to cerebellum ratios of approx. 2 between 30 and 60 mins. Our experiments have been carried out with the racemic mixture. We are currently in the process of preparing the pure (*S*)-enantiomer of the aminotetralins which are known to have a higher affinity for the D2/D3 receptors [12]. The use of the pure isomer is expected to reduce nonspecific binding in both the cortex and cerebellum and thus improve the quality of the imaging data.

Competition of the binding of  $^{18}\text{F}$ -5-OH-FPPAT was carried out with risperidone (a dopamine D2 receptor antagonist) and PPHT (a dopamine D2 receptor agonist). Compared to the control rats, both the agents reduced the binding of  $^{18}\text{F}$ -5-OH-FPPAT to the striata approx. to a similar extent (Fig. 5b). These findings suggest the reversibility of  $^{18}\text{F}$ -5-OH-FPPAT with an antagonist and agonist. The use of the pure isomer rather than the racemic mixture is likely to improve the sensitivity of these measurements by lowering the nonspecific binding.

In vivo binding of  $^{18}\text{F}$ -5-OH-FPPAT in the primate brain was evaluated by PET. Localization of  $^{18}\text{F}$ -5-OH-FPPAT was evident in the caudate and putamen while it cleared out from the cortex and cerebellum. Fig. 6 shows PET image slices of the monkey brain indicative of the selective binding of  $^{18}\text{F}$ -5-OH-FPPAT to the dopaminergic regions. The images also reveal some binding in the thalamus which needs to be further investigated by the use of the pure (*S*)-isomer. These findings are similar to our previous results on  $^{11}\text{C}$ -5-OH-DPAT [2]. Thus,  $^{18}\text{F}$ -5-OH-FPPAT is a good fluorine-18 radiolabeled analog of  $^{11}\text{C}$ -5-OH-DPAT.

Uptake of  $^{18}\text{F}$ -5-OH-FPPAT was rapid and high and is comparable to  $^{11}\text{C}$ -5-OH-DPAT. Time-activity curves of the localization of  $^{18}\text{F}$ -5-OH-FPPAT (Fig. 7) shows selectivity for the putamen and caudate over the cortex and cerebellum. Some selective binding in the thalamus was also observed which exhibited slower clearance compared to cortex and cerebellum. A ratio of approximately 2 between striata and cerebellum was seen and is evident that the localization of  $^{18}\text{F}$ -5-OH-FPPAT is dopamine D2/D3 receptor mediated. It must be noted that all experiments have been carried out with the racemic (*R,S*)- $^{18}\text{F}$ -5-OH-FPPAT. Since it is known that the (*S*)-isomer of 5-hydroxyaminotetralins has higher affinity than the (*R*)-isomer, the radiolabeling of the pure (*S*)-isomer of  $^{18}\text{F}$ -5-OH-FPPAT may result in a higher target to nontarget ratios. Thus,

$^{18}\text{F}$ -5-OH-FPPAT appears to be a promising fluorine-18 radiolabeled agonist imaging agent for dopamine D2/D3 receptors.

## 5. Conclusions

We have successfully prepared a fluorinated high affinity dopamine D2/D3 receptor agonist,  $^{18}\text{F}$ -5-OH-FPPAT. This new radiotracer binds predominantly to the HA-state of the D2 receptors in vitro in rat brain slices. This is one of the few, fluorinated dopamine D2/D3 receptor agonists known to be able to successfully localize in dopaminergic regions. We have shown selective binding of this radiotracer to the dopamine D2 receptors in vivo and demonstration of the binding to the HA-state in vitro. Long half-life fluorine-18 label will allow extensive in vitro studies. The successful development of the D2 receptor agonist PET radiotracer should allow the analysis of a subpopulation of the D2 receptors more accurately than has been previously possible.

## Acknowledgments

This research was supported by the Biological and Environmental Program (BER), U.S. Department of Energy, Grant No. DE-FG03-02ER63294. We like to thank Dr. Martin Satter for technical assistance. We like to thank Dr. Harold Stills and his Staff for assistance with the non-human primates.

## References

- [1] Shi B, Narayanan TK, Yang ZY, Christian BT, Mukherjee J. Radio-synthesis and *in vitro* evaluation of 2-(N-alkyl-N-1- $^{11}\text{C}$ -propyl)-amino-tetralin analogs as high affinity dopamine D-2 receptor agonists for use as potential PET radiotracers. Nucl Med Biol 1999;26:725–35.
- [2] Mukherjee J, Narayanan TK, Shi B, Christian BT, Dunigan KA, Mntil J. *In vitro* and *in vivo* evaluation of the binding of the dopamine D-2 receptor agonist,  $^{11}\text{C}$ -(R,S)-5-hydroxy-2-(di-n-propylamino)-tetralin in rodents and non-human primate. Synapse 2000;37:70.
- [3] Mukherjee J, Christian BT, Shi B, Narayanan TK. Comparison of dopamine D-2 receptor agonists,  $^{11}\text{C}$ -5-OH-DPAT,  $^{11}\text{C}$ -PPHT,  $^{11}\text{C}$ -ZYY339 and  $^{18}\text{F}$ -5-OH-FPPAT as *in vivo* imaging agents for PET. J Nucl Med 2000;41:94.
- [4] Cumming P, Wong DF, Gillings N, Hilton J, Scheffel U, Gjedde A. Specific binding of [ $^{11}\text{C}$ ]raclopride and N-[ $^3\text{H}$ ]propyl-norapomorphine to dopamine receptors in living mouse striatum: Occupancy by endogenous dopamine guanosine triphosphate-free G protein. J. Cereb Blood Flow Metab 2002;22:596–604.
- [5] Hwang D-R, Kegeles LS, Laruelle M. (-)-N-[ $^{11}\text{C}$ ]Propyl-norapomorphine: a positron-labeled dopamine agonist for PET imaging of D-2 receptors. Nucl Med Biol 2000;27:533–9.
- [6] Ross SB, Jackson DM. Kinetic properties of the *in vivo* accumulation of  $^3\text{H}$ -N-n-propylapomorphine in the mouse brain. Naunyn Schmied-eder Arch Pharmacol 1989;340:13–20.
- [7] Zijlstra S, Elsinga PH, Oosterhuis EZ, Visser GM, Korf J, Vaalburg W. Synthesis and *in vivo* distribution in the rat of several fluorine-18 labeled 5-hydroxy-2-aminotetralin derivatives. Appl Radiat Isot 1993;44:473–80.
- [8] Mukherjee J, Yang ZY, Das MK, Brown T. Fluorinated benzamide neuroleptics 3. Development of (S)-N-[(1-allyl-2-pyrrolidinyl)methyl]-5-(3[F-18]fluoropropyl)-2, 3-dimethoxybenzamide as an improved dopamine D-2 receptor tracer. Nucl Med Biol 1995;22:283–96.
- [9] Grigoriadis D. and Seeman, P. Complete conversion of brain D-2 dopamine receptors from the high- to low-affinity state for dopamine agonists, using sodium ions and guanine nucleotide. J Neurochem 1985;44:1925–35.
- [10] Vessotskie JM., Kung M-P., Chumpradit S., Kung H. F. Characterization of [ $^{125}\text{I}$ ]S(-)-5-OH-PIPAT binding to dopamine D-2 like receptors expressed in cell lines. Neuropharmacology 1997;36:999–1007.
- [11] Nobrega JN., Seeman P. Dopamine D-2 receptors mapped in rat brain with  $^3\text{H}$ (+)PHNO. Synapse 1994;17:167–72.
- [12] Karlsson A., Bjork L., Pettersson C., Anden NE., Hacksell U. (R)- and (S)-5-hydroxy-2-(dipropylamino)tetralin (5-OH-DPAT): assessment of optical purities and dopaminergic activities. Chirality 1990; 2:90–5.

[1] Shi B, Narayanan TK, Yang ZY, Christian BT, Mukherjee J. Radio-synthesis and *in vitro* evaluation of 2-(N-alkyl-N-1- $^{11}\text{C}$ -propyl)-ami-